Reduced Kinetic Mechanisms and Their Numerical Treatment I: Wet CO Flames

W. WANG and B. ROGG*

University of Cambridge, Department of Engineering, Trumpington Street, Cambridge CB2 1PZ, England

In the present article we investigate laminar, premixed freely propagating wet CO flames, i.e., flames whose initial mixture contains small amounts of hydrogen and water vapor. Attention is focused on the derivation and validation of reduced kinetic schemes that provide both more computational efficiency in the calculation and the basis for asymptotic analysis of such flames. Specifically, a short detailed mechanism and systematically reduced three-step, two-step, and one-step mechanisms are derived that allow realistic predictions of burning velocities and flame structures over a wide range of stoichiometries. *Inner iteration* is discussed in detail and its *black box* character is identified. Also presented and discussed are numerical tricks for efficient use of reduced kinetic mechanisms in flame calculations. In particular, the so-called *partially explicit* numerical schemes are identified.

1. INTRODUCTION

Although deflagrations of dry mixtures of carbon monoxide and oxygen can occur at sufficiently high pressures, under practical conditions there are sufficiently large amounts of hydrogen-containing species present for the elementary kinetic step $OH + CO \rightarrow CO_2 + H$ to dominate hydrogen-free steps. Thus, there is practical interest in investigating deflagrations in wet CO mixtures. Moreover, in wet CO flames of low hydrogen content the hydrogen-containing species may be expected to achieve steady states and, thereby, produce a one-step reduced mechanism that describes the flame propagation with high accuracy. Therefore, the wet CO flames addressed in the present paper offer a unique testing ground for reduced mechanisms.

Wet CO flames were studied previously. Lewis and von Elbe [1] report extensive experimental data on burning velocities of CO–O_2–N_2 mixtures with small amounts of H_2 and H_2O added. With the aim of establishing detailed kinetic mechanisms, numerical studies of premixed CO flames with varying H_2 and H_2O initial concentrations were carried out for stoichiometric flames by Warnatz [2], and for a range of stoichiometries by Dixon-Lewis and coworkers [3–5]. Rogg and Williams [6] reduced the chemistry of wet CO flames to a three-step mechanism that gave reasonable agreement with predictions of a full kinetic mechanism comprising 67 elementary steps among 12 reacting species. In Ref. 7 prospects for the derivation of a two-step mechanism were given. In the present article we present and derive, respectively, two detailed and several reduced kinetic mechanisms. Specifically, taking a short detailed kinetic mechanism as the starting point, we derive three-step, two-step, and one-step kinetic mechanisms for wet CO flames. The results for burning velocity and flame structure obtained with the various kinetic mechanisms are compared with each other and to experimental data available in the literature. The numerical treatment of the reduced mechanisms is discussed in detail. In particular, tricks for flame computations with reduced mechanisms in general, that is, tricks not restricted to wet CO flames, are presented and discussed.

2. THE GOVERNING EQUATIONS AND THEIR NUMERICAL SOLUTION

The steady, planar, adiabatic deflagration is considered, and the subscripts u and b identify conditions in the unburnt and burnt gas,

*Author to whom correspondence should be addressed.

Copyright © 1993 by The Combustion Institute
Published by Elsevier Science Publishing Co., Inc.

0010-2180/93/$6.00

respectively. Mass conservation is $\rho v = \rho_u v_u$, where v_u is the laminar burning velocity which must be determined as part of the solution. The conservation equations for energy and species mass are

$$\rho v \frac{dT}{dx} = \frac{1}{c_p}\frac{d}{dx}\left(\lambda \frac{dT}{dx}\right) - \frac{dT}{dx}\sum_{i=1}^{N}\left(\frac{c_{pi}}{c_p}\rho Y_i V_i\right) - \frac{1}{c_p}\sum_{i=1}^{N} h_i w_i, \quad (1)$$

$$\rho v \frac{dY_i}{dx} = -\frac{d}{dx}(\rho Y_i V_i) + w_i, \quad i = 1, \ldots, N-1, \quad (2)$$

where Y_i is the mass fraction of species i, V_i its diffusion velocity, w_i its mass rate of production and h_i its enthalpy of formation at temperature T. There are N chemical species in the mixture, and Eq. 2 is applied to $N-1$ of them, the concentration of the inert N_2 being obtained by difference. Boundary conditions for Eqs. 1 and 2 are

$$T = T_u, \quad Y_i = Y_{iu}, \quad i = 1, \ldots, N-1 \quad \text{at } x = -\infty,$$
$$dT/dx = dY_i/dx = 0, \quad i = 1, \ldots, N-1 \quad \text{at } x = \infty. \quad (3)$$

Since details of the transport model and further references for it may be found in Ref. 8, only a short summary is given here. The diffusion approximations recommended by Hirschfelder and Curtiss [9] were adopted, with Soret effects included but Dufour effects neglected, since Clavin and coworkers [10] have shown that, although the latter generally is unimportant, the former can influence flame behavior through its influence on the temperature at the reaction zone. The diffusion coefficients needed to calculate the V_i vary with temperature and composition and were evaluated from molecular data; the thermal conductivity λ and specific heat capacities at constant pressure, c_{pi} and c_p, were obtained similarly, as described by Rogg [8].

With the chemistry models specified in the following sections, the governing Eqs. 1 and 2 were solved with the commercial Cambridge laminar-flame computer code RUN-1DL [11] which has been used for the numerical simulation of premixed burner-stabilized and freely propagating flames, strained premixed, nonpremixed and partially premixed flames subject to a variety of boundary conditions, spherical flames and tubular flames (see, e.g., Refs. 12–15). RUN-1DL employs fully self-adaptive gridding [16, 17]; it solves both transient [16, 18] and steady-state problems in physical space and for diffusion flames, alternatively, in mixture-fraction space [19]. For the calculations reported herein, of the various numerical solvers that are implemented in RUN-1DL a modified Newton method has been selected. For further details of the computer code and the selected numerical-solution method the cited papers should be consulted. Numerical issues that are specific to calculations with systematically reduced kinetic mechanisms are discussed below in section 8.

3. DETAILED KINETIC MECHANISMS

In the present article two detailed kinetic mechanisms are employed. The first, termed the "full mechanism," is a subset of the detailed mechanism for C–H–O–N systems presented in chapter 1 of Ref. 20. The full mechanism is shown in Table 1. The second detailed kinetic mechanism is termed the "short mechanism"; it is obtained from the full mechanism by disregarding step 5b, which has a particularly large activation energy, steps 11 to 14b, in which H_2O_2 is either formed or consumed, as well as the recombination step 17, and steps 22 and 23. In Table 1, the numbers of those reactions not contained in the short mechanism are written in parentheses. The short mechanism comprises ten reacting species and three elements.

For all flames computed herein, boundary conditions and parameters were selected to correspond to the experiments reported by Lewis and von Elbe [1]. Thus, atmospheric pressure and an initial temperature of 300 K were adopted, and the fuel was assumed to contain fixed molar percentages of CO (97.15%), H_2 (1.5%) and H_2O (1.35%). Parameters varied systematically in the computations are the initial $O_2/(N_2 + O_2)$ molar ratio, f,

TABLE 1

Detailed Mechanism and Rate Data for Wet CO Flames in units of mol, cm, s, kJ, and K[a]

No.	Reaction			A	α	E
			H_2/O_2 Chain Reactions			
1f	$O_2 + H$	→	$OH + O$	2.000E + 14	0.00	70.30
1b	$OH + O$	→	$O_2 + H$	1.568E + 13	0.00	3.52
2f	$H_2 + O$	→	$OH + H$	5.060E + 04	2.67	26.30
2b	$OH + H$	→	$H_2 + O$	2.222E + 04	2.67	18.29
3f	$H_2 + OH$	→	$H_2O + H$	1.000E + 08	1.60	13.80
3b	$H_2O + H$	→	$H_2 + OH$	4.312E + 08	1.60	76.46
4f	$OH + OH$	→	$H_2O + O$	1.500E + 09	1.14	0.42
4b	$H_2O + O$	→	$OH + OH$	1.473E + 10	1.14	71.09
			HO_2 Formation and Consumption			
5f	$O_2 + H + M'$	→	$HO_2 + M'$	2.300E + 18	−0.80	0.00
(5b)	$HO_2 + M'$	→	$O_2 + H + M'$	3.190E + 18	−0.80	195.39
6	$HO_2 + H$	→	$OH + OH$	1.500E + 14	0.00	4.20
7	$HO_2 + H$	→	$H_2 + O_2$	2.500E + 13	0.00	2.90
8	$HO_2 + OH$	→	$H_2O + O_2$	6.000E + 13	0.00	0.00
9	$HO_2 + H$	→	$H_2O + O$	3.000E + 13	0.00	7.20
10	$HO_2 + O$	→	$OH + O_2$	1.800E + 13	0.00	−1.70
			H_2O_2 Formation and Consumption			
(11)	$HO_2 + HO_2$	→	$H_2O_2 + O_2$	2.500E + 11	0.00	−5.20
(12f)	$OH + OH + M'$	→	$H_2O_2 + M'$	3.250E + 22	−2.00	0.00
(12b)	$H_2O_2 + M'$	→	$OH + OH + M'$	1.692E + 24	−2.00	202.29
(13)	$H_2O_2 + H$	→	$H_2O + OH$	1.000E + 13	0.00	15.00
(14f)	$H_2O_2 + OH$	→	$H_2O + HO_2$	5.400E + 12	0.00	4.20
(14b)	$H_2O + HO_2$	→	$H_2O_2 + OH$	1.802E + 13	0.00	134.75
			Recombination Reactions			
15	$H + H + M'$	→	$H_2 + M'$	1.800E + 18	−1.00	0.00
16	$OH + H + M'$	→	$H_2O + M'$	2.200E + 22	−2.00	0.00
(17)	$O + O + M'$	→	$O_2 + M'$	2.900E + 17	−1.00	0.00
			CO/CO_2 Mechanism			
18f	$CO + OH$	→	$CO_2 + H$	4.400E + 06	1.500	−3.10
18b	$CO_2 + H$	→	$CO + OH$	4.956E + 08	1.500	89.76
			HCO Consumption			
21	$HCO + H$	→	$CO + H_2$	2.000E + 14	0.00	0.00
(22)	$HCO + OH$	→	$CO + H_2O$	1.000E + 14	0.00	0.00
(23)	$HCO + O_2$	→	$CO + HO_2$	3.000E + 12	0.00	0.00
24f	$HCO + M'$	→	$CO + H + M'$	7.100E + 14	0.00	70.30
24b	$CO + H + M'$	→	$HCO + M'$	1.136E + 15	0.00	9.97

[a]The third-body efficiencies with respect to molecular hydrogen are 6.5 for CH_4, 6.5 for H_2O, 1.5 for CO_2, 0.75 for CO, 0.4 for O_2, 0.4 for N_2, and 1.0 for all other species. The mechanism is a subset of the mechanism given in chapter 1 of Ref. 20. Reactions, whose reaction numbers are in parentheses, are absent in the short mechanism.

and the initial fuel mole fraction in the mixture, X_{fuel}.

The numerical results obtained for flame structures and burning velocities using the full and, alternatively, the short kinetic mechanism are in excellent agreement. Shown in Fig. 1 is the burning velocity as a function of the initial fuel mole fraction for $f = 0.13$, 0.21, 0.4, and 0.985. In Fig. 1 symbols represent experimental data taken from Lewis and von Elbe [1], dotted lines refer to computational results obtained with the full mechanism, and dashed lines to

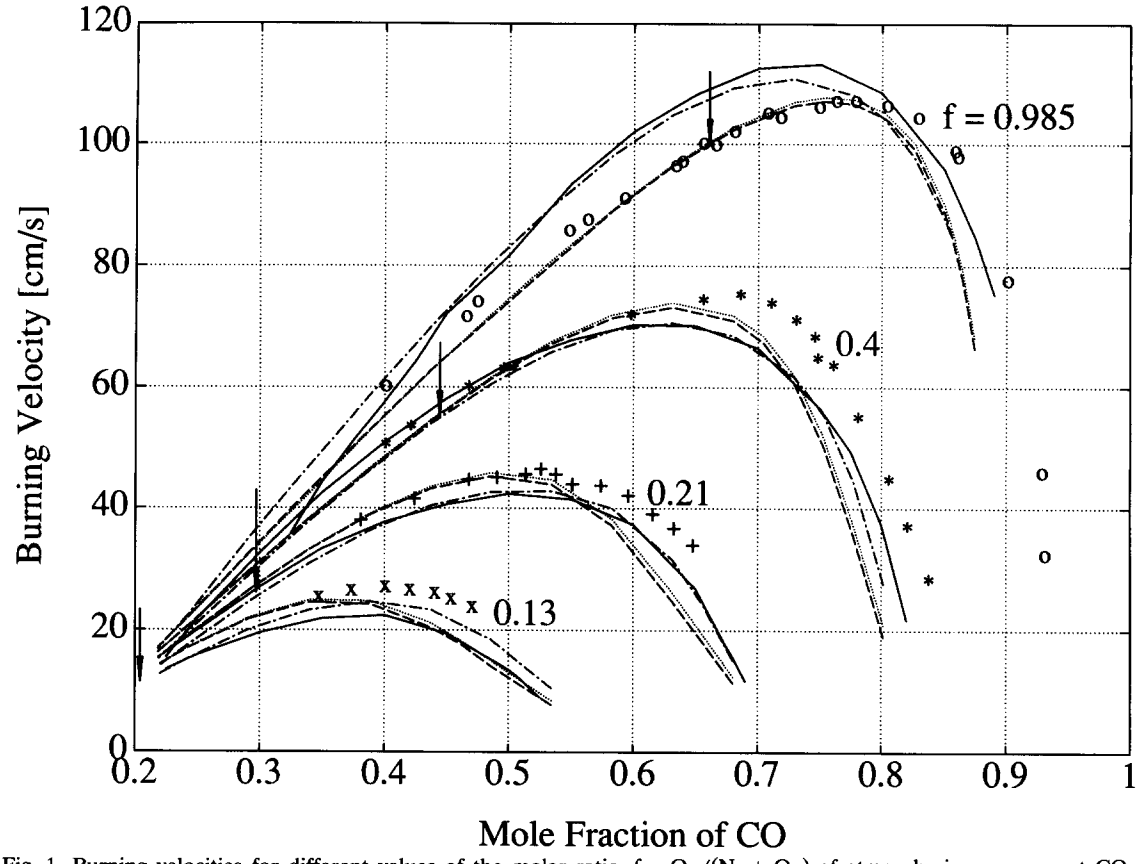

Fig. 1. Burning velocities for different values of the molar ratio $f = O_2/(N_2 + O_2)$ of atmospheric-pressure wet CO flames as a function of the initial mole fraction of CO. Symbols: experimental data from Ref. 1. Lines: computational results; dotted lines: full mechanism; dashed lines: short mechanism; dashed-dotted lines: two-step reduced mechanism; solid lines: one-step reduced mechanism. Vertical arrows identify stoichiometric initial composition.

computational results obtained with the short mechanism. The dashed-dotted and solid lines can be ignored for the moment because they represent results obtained with a two-step mechanism and a one-step mechanism, respectively, that will be derived below. The vertical arrows in Fig. 1 identify stoichiometric initial composition. Shown in Figs. 2–4 are structures of wet CO–air flames ($f = 0.21$) calculated with the short mechanism. Since over the entire range of stoichiometries the short mechanism is found to produce flame-structure results that agree very well with those of the full mechanism, results obtained with the latter mechanism are not shown here. Figure 2 is for a stoichiometric flame ($X_{fuel} = 0.3$), Fig. 3 for a moderately rich flame ($X_{fuel} = 0.5$), and Fig. 4 for a very rich flame ($X_{fuel} = 0.65$). In the following the short mechanism will be taken as the starting point for the derivation of a three-step, a two-step, and a one-step reduced kinetic mechanism. The burning velocities and flame structures obtained with the short mechanism will serve as benchmark solutions against which the reduced mechanisms will be validated.

4. THREE BASIC INGREDIENTS OF SYSTEMATICALLY REDUCED KINETIC MECHANISMS

Prior to proceeding it appears appropriate to give a short review of the three basic ingredients of systematically reduced kinetic mechanisms, viz., (i) the steady-state approximation, (ii), truncation, and (iii), inner iteration. The systematical derivation of reduced kinetic mechanisms necessitates a thorough understanding of the *steady-state approximation*. This approximation, and also the partial-

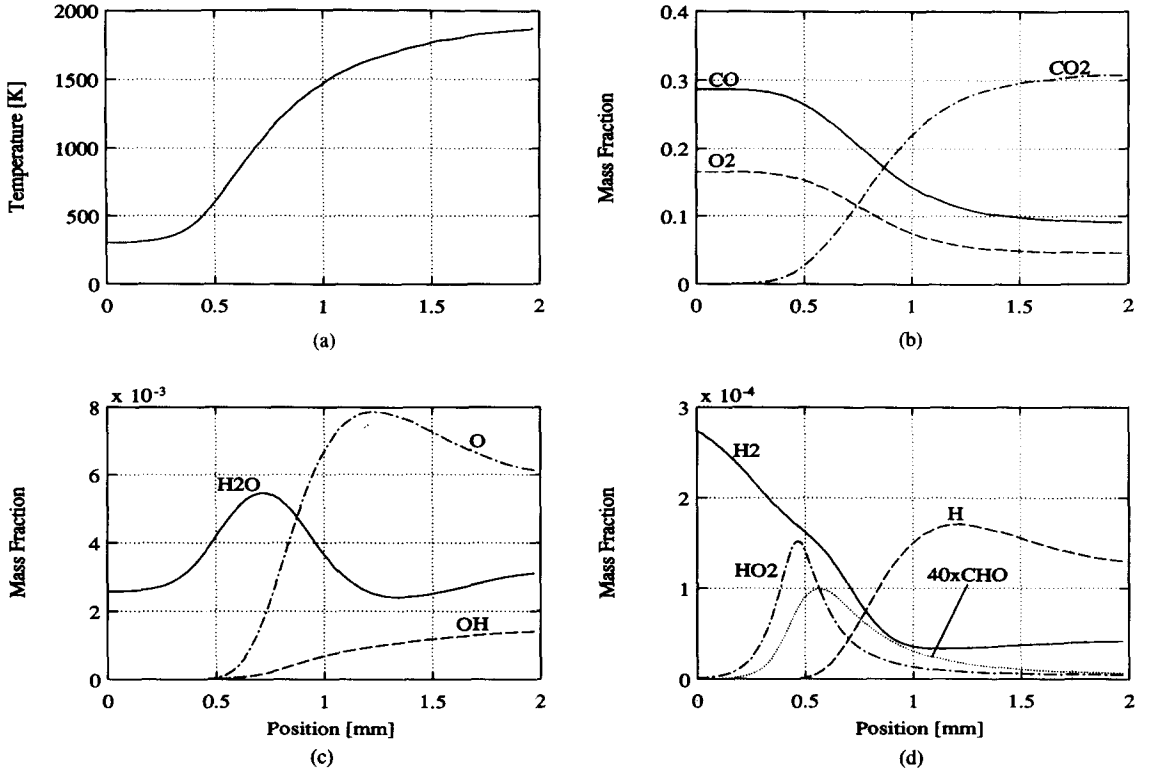

Fig. 2. Temperature and species mass-fraction profiles of a stoichiometric atmospheric-pressure wet CO–air flame calculated with the short mechanism. The initial mole fraction of the fuel (CO: 97.15%, H_2: 1.5% and H_2O: 1.35%) is 0.3.

equilibrium approximation, is discussed in a general manner in detail by Williams [21, pp. 565–570, pp. 172–173, pp. 174–177]. A discussion of both approximations with specific reference to H_2–O_2–N_2 mixtures is given by Dixon-Lewis, [22]. In the derivation of reduced kinetic mechanisms, steady-state approximations are introduced for essentially two reasons, viz.,

to reduce the number of chemical species for which species conservation equations, i.e., equations of the kind of Eq. 2, need to be solved numerically. This can give substantial savings in computer time, in particular for time dependent and/or spatially multidimensional problems.

to remove stiffness from the governing equations thereby increasing computational efficiency.

At this point it is worthwhile to note that for the same two reasons in the past various research groups have used partial-equilibrium approximations. However, it was found that, in general, the validity of partial-equilibrium assumptions is more restricted than that of steady-state assumptions and, therefore, their usefulness generally is limited to truncation, which is discussed next.

Usually steady-state approximations result in algebraically complicated equations which must be solved for the concentrations of those species for which steady states have been assumed. This is where a process termed truncation comes in. In truncation, certain terms in the steady-state expressions are deleted

to achieve simplifications which aid in solving the often complicated, nonlinear algebraic system of steady-state relationships, and

to achieve fine tuning such that the reduced mechanism yields even more realistic flame structures and, in the case of premixed flames, burning velocities.

Often partial equilibria are applied in truncation methods. Furthermore, we note that

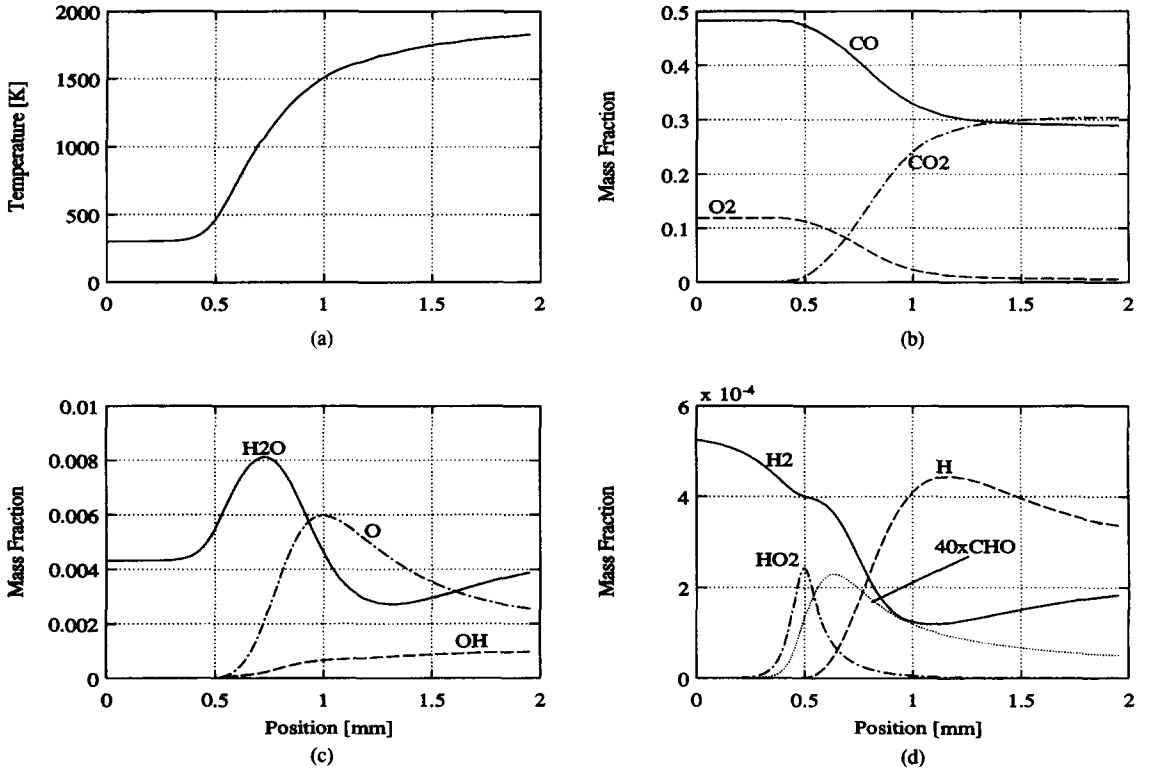

Fig. 3. As Fig. 2, but with an initial mole fraction of fuel of 0.5.

steady-state approximations which have been simplified by truncation are also referred to as "truncated steady states"; steady-state approximations with no further simplifications are also referred to as "full steady states."

Although truncation represents an important process in the derivation of reduced kinetic mechanisms, of course there are limits to which it can be employed without loss of quality in the prediction of flame structure. Thus, despite of simplifications achieved by truncation, usually nonlinear, algebraic systems of equations, which result from steady-state approximations, need to be solved for the concentrations of the steady-state species. This is where inner iteration comes in.

Historically the adjective "inner" of inner iteration was introduced to distinguish between the iterative solution, say by Newton's method, of the equations governing the conservation of overall mass, momentum, energy, and species mass from the iteration required to solve the aforementioned nonlinear, algebraic systems of equations for the concentrations of the steady-state species. Thus, within each iteration step of the Newton method, say, "inner iterations" were performed to obtain the concentrations of the steady-state species that are required to evaluate the global rates of a systematically reduced mechanism. Of course, a method for the numerical integration of the conservation equations of overall mass, species mass, momentum, and energy needs not to be iterative; it may well be a noniterative method such as the PISO method [23] or one of the methods described in section 8. Nevertheless, if an iterative approach is required to solve the nonlinear system of equations governing the concentrations of the steady-state species, this approach is referred to as "inner" iteration. In the present paper inner iteration has been employed in the calculations using both the two-step and the one-step mechanism. For the latter mechanism the numerical realization of inner iteration is described in detail in subsection 7.4. The interested reader may also consult Ref. 24.

Various useful tools can be used to derive systematically reduced kinetic mechanisms. For instance, much of the linear algebra resulting

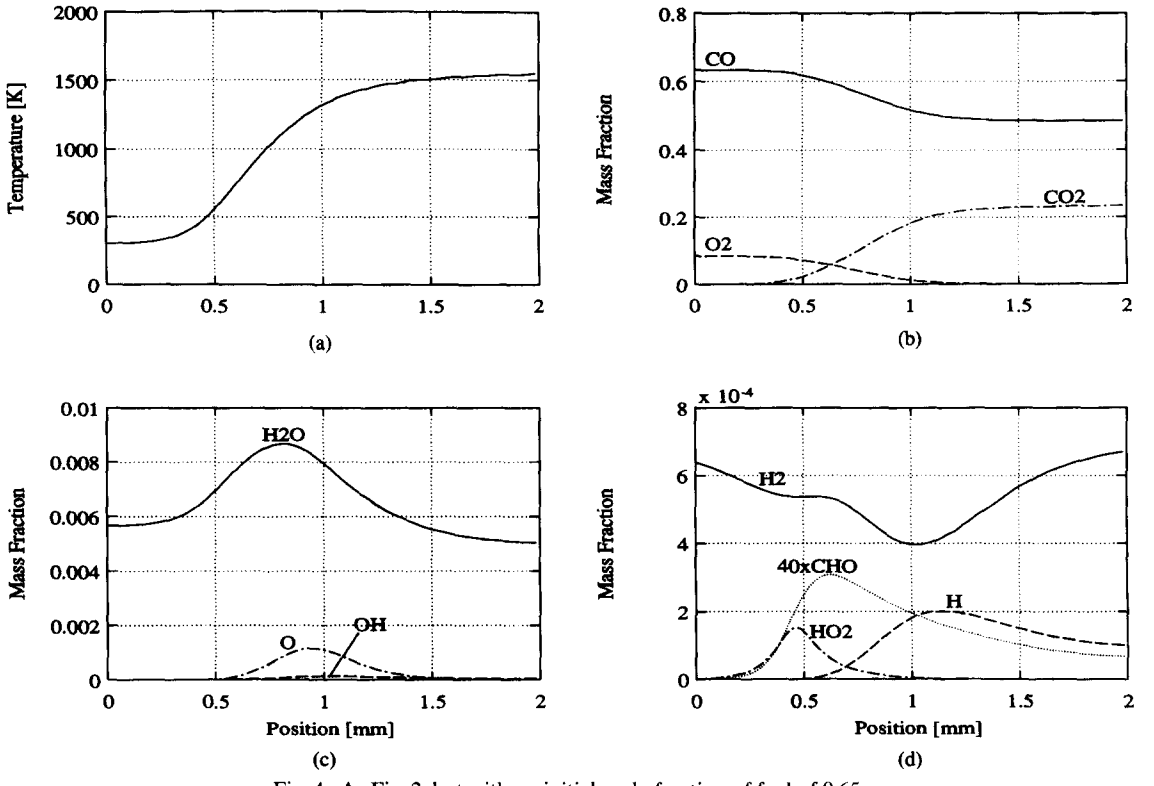

Fig. 4. As Fig. 2, but with an initial mole fraction of fuel of 0.65.

from steady-state approximations can be left to small computer programs, such as the one developed by Göttgens and Terhoeven [25]. Another useful tool which, for instance, helps to identify important reactions in a kinetic mechanism or aids in the fine tuning by truncation, is sensitivity analysis, [26]. Finally, it is important to point out that whatever assumptions and approximations are made in deriving a reduced kinetic mechanism, either with or without aiding tools, the validity of these assumptions and approximations needs to be verified, at least *a posteriori*.

5. A THREE-STEP MECHANISM

In an earlier paper [7] on wet CO flames, possible steady states and partial equilibria were tested. It was found that all reaction intermediates maintain good steady states for lean flames, although the approximations become poor for H, H_2 and H_2O at very rich conditions. Furthermore it was found that although step 1 of Table 1 maintains the best partial equilibrium for lean flames, over the full range of stoichiometry step 3, at balance, is best. Therefore, in the present study partial-equilibrium approximations will not be used in the derivation of reduced mechanisms.

Since there are seven independent chemical species in the short mechanism, with four species in steady state, a three-step kinetic mechanism is obtained. If HCO, O, OH, and HO_2 are selected as the steady-state species, the three-step mechanism

$$CO + H_2O \rightleftharpoons CO_2 + H_2, \quad \text{(I)}$$

$$2H + M \rightarrow H_2 + M, \quad \text{(II)}$$

$$O_2 + 3H_2 \rightleftharpoons 2H_2O + 2H \quad \text{(III)}$$

can be derived. In this mechanism, step I is the overall CO consumption step which neither creates nor destroys reaction intermediaries. Step II represents an overall recombination step, and step III an overall radical-production, oxygen-consumption step. Note that this three-step mechanism is formally identical to that derived by Rogg and

Williams [6] for wet CO flames and by Chen et al. [27] for CO/air diffusion flames. In terms of the rates of the elementary steps contained in the short mechanism, the global rates of the three-step mechanism can be written as

$$\omega_I = \omega_{18f} - \omega_{18b}, \tag{4}$$

$$\omega_{II} = \omega_{5f} + \omega_{15} + \omega_{16} - \omega_{24f} + \omega_{24b}, \tag{5}$$

$$\omega_{III} = \omega_{1f} - \omega_{1b} + \omega_6 + \omega_9. \tag{6}$$

Since derivation of a three-step mechanism for wet CO flames was discussed in detail in Ref. 6, herein it is not considered further. Instead, subsequently the three-step mechanism is used as the basis for further reduction.

6. A TWO-STEP MECHANISM

6.1 Derivation of the Two-Step Mechanism

If H atoms are assumed to be in steady state, the above three-step mechanism becomes a two-step mechanism which, after standard manipulations, can be written as

$$CO + H_2O \rightleftharpoons CO_2 + H_2, \tag{I'}$$

$$2H_2 + O_2 \rightarrow 2H_2O. \tag{II'}$$

Here step I' is the overall CO consumption step which is identical with step I of the three-step mechanism, and step II' is an overall oxygen consumption step. The water and hydrogen consumed in the two global steps represent both the catalysts present in the fresh, unburnt mixture and the products of chemical reaction. The global rates of the two-step mechanism are formally identical to the rates of steps I and III of the above three-step mechanism, i.e., they are given by

$$\omega_{I'} = \omega_{18f} - \omega_{18b}, \tag{7}$$

$$\omega_{II'} = \omega_{1f} - \omega_{1b} + \omega_6 + \omega_9. \tag{8}$$

In the elementary rates appearing on the right-hand sides of Eqs. 7 and 8, the concentrations of the steady-state species must be expressed in terms of the concentrations of the species appearing explicitly in the two-step mechanism. Therefore, the global rates are algebraically more or less complex expressions containing rate data of many of the elementary steps of the short mechanism; the degree of complexity of the global rates depends, of course, on the specific assumptions introduced in their derivation.

In the following we assume that the concentrations of the species appearing explicitly in the two-step mechanism, that is, [CO], [O_2], [H_2], [CO_2], and [H_2O], are known by solving numerically the governing equations 1 and 2. The concentrations of the steady-state species H, OH, O, HO_2, and HCO, which do not appear explicitly in the reduced mechanism but are required to evaluate the global rates according to Eqs. 7 and 8, are expressed in terms of the known species concentrations as follows.

Based on extensive numerical explorations and sensitivity analysis, herein full steady states are adopted for HO_2 and HCO, and truncated steady states for H atoms, O atoms and the OH radical. Specifically, in the steady-state relationship for H atoms the elementary steps 6, 9, 15, and 16 are omitted, in that for O atoms step 9, and in that for OH radical steps 8 and 10. The resulting steady-state relationships are, in the order H, OH, O, HO_2, and HCO,

$$\begin{aligned} 0 = {} & \omega_{1f} - \omega_{1b} - \omega_{2f} + \omega_{2b} - \omega_{3f} \\ & + \omega_{3b} + \omega_{5f} + \omega_7 \\ & - \omega_{18f} + \omega_{18b} + \omega_{21} - \omega_{24f} + \omega_{24b}, \end{aligned} \tag{9}$$

$$\begin{aligned} 0 = {} & \omega_{1f} - \omega_{1b} + \omega_{2f} - \omega_{2b} - \omega_{3f} \\ & + \omega_{3b} - 2\omega_{4f} + 2\omega_{4b} \\ & + 2\omega_6 - \omega_{16} - \omega_{18f} + \omega_{18b}, \end{aligned} \tag{10}$$

$$\begin{aligned} 0 = {} & \omega_{1f} - \omega_{1b} - \omega_{2f} + \omega_{2b} \\ & + \omega_{4f} - \omega_{4b} - \omega_{10}, \end{aligned} \tag{11}$$

$$0 = \omega_{5f} - \omega_6 - \omega_7 - \omega_8 - \omega_9 - \omega_{10}, \tag{12}$$

$$0 = \omega_{21} + \omega_{24f} - \omega_{24b}. \tag{13}$$

Equations 9–13 can be solved for the concentrations of the steady-state species, viz.,

$$[H] = \frac{N}{D}, \tag{14}$$

$$N = k_{1b}[O][OH] + k_{2f}[H_2][O] + k_{3f}[H_2][OH] + k_{18f}[CO][OH] + k_{24f}[HCO][M],$$

$$D = k_{1f}[O_2] + k_{2b}[OH] + k_{3b}[H_2O] + k_{5f}[M][O_2] + k_7[HO_2] + k_{18b}[CO_2] + k_{21}[HCO] + k_{24b}[CO][M],$$

$$[OH] = \frac{N}{D}, \tag{15}$$

$$N = k_{1f}[H][O_2] + k_{2f}[H_2][O] + k_{3b}[H][H_2O] + 2k_{4b}[H_2O][O] + 2k_6[H][HO_2] + k_{18b}[CO_2][H],$$

$$D = k_{1b}[O] + k_{2b}[H] + k_{3f}[H_2] + 2k_{4f}[OH] + k_{16}[H][M] + k_{18f}[CO], \tag{16}$$

$$[O] = \frac{k_{1f}[H][O_2] + k_{2b}[H][OH] + k_{4f}[OH]^2}{k_{1b}[OH] + k_{2f}[H_2] + k_{4b}[H_2O] + k_{10}[HO_2]},$$

$$[HCO] = \frac{k_{24b}[CO][H][M]}{k_{21}[H] + k_{24f}[M]}, \tag{17}$$

$$[HO_2] = \frac{k_{5f}[H][O_2][M]}{k_6[H] + k_7[H] + k_8[OH] + k_9[H] + k_{10}[O]}. \tag{18}$$

Inspection of Eqs. 14–18 shows that some of these equations are strongly coupled and, therefore, must be solved by inner iteration. For a detailed discussion of the technique of inner iteration section 4 of the present paper and Ref. 24 should be consulted; in the context of the results obtained for a one-step mechanism, further details on inner iteration, in particular regarding its numerical realization, are given in subsection 7.4. In order to start the inner iteration for the present problem, the initial concentration of H is prescribed as 10^{-10}; the initial concentrations of OH and O are calculated by assuming partial equilibrium for reactions 2 and 3, that is, from the relationships

$$[OH] = \frac{k_{3b}[H][H_2O]}{k_{3f}[H_2]}, \tag{19}$$

$$[O] = \frac{k_{2b}[OH][H]}{k_{2f}[H_2]}. \tag{20}$$

It is emphasized here that these partial equilibria are only starting guesses for the inner iteration and are not present in the final results.

6.2. Results for Burning Velocities and Flame Structures

Shown in Fig. 1 as dashed-dotted lines is the burning velocity as a function of the initial CO mole fraction X_{fuel} for values of the molar ratio f of 0.13, 0.21, 0.4, and 0.985. It is seen that for all stoichiometries and even the highest value of f, which corresponds to nearly no nitrogen and the highest flame temperatures, burning velocities obtained from the two-step mechanism are in excellent to good agreement with those obtained from the detailed mechanisms. It is also seen that for very rich conditions the burning velocities calculated with the two-step mechanism agree better with the experimental data than those obtained with the detailed mechanisms.

Shown in Figs. 5–7 are numerical results for flame structures obtained with the two-step mechanism. Figure 5 is for a stoichiometric flame ($X_{\text{fuel}} = 0.3$), Fig. 6 for a moderately rich flame ($X_{\text{fuel}} = 0.5$), and Fig. 7 for a very rich flame ($X_{\text{fuel}} = 0.65$). Comparison of Figs. 5–7 with the corresponding results obtained with the short mechanism (see Figs. 2–4) shows that the temperatures in the hot portions of the flame as calculated with the two-step

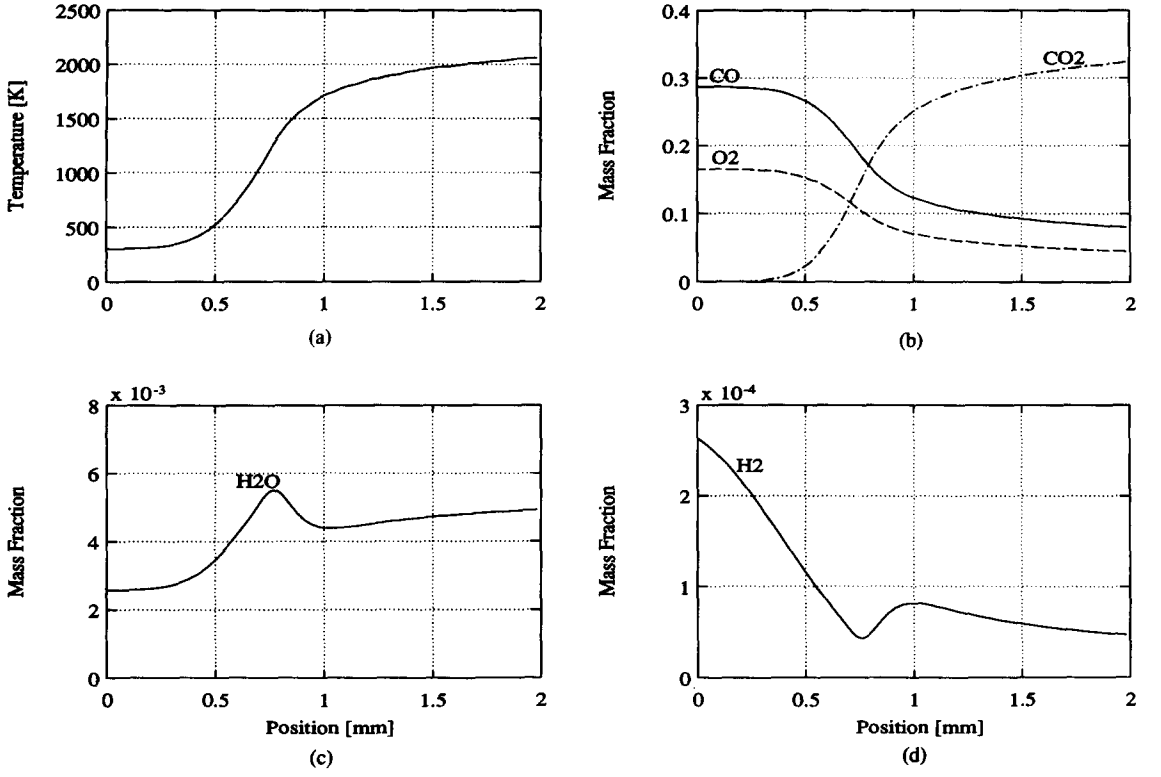

Fig. 5. Temperature and species mass-fraction profiles of a stoichiometric atmospheric-pressure wet CO–air flame calculated with the two-step mechanism. The initial mole fraction of the fuel (CO: 97.15%, H_2: 1.5% and H_2O: 1.35%) is 0.3.

mechanism are higher for the stoichiometric and the moderately rich flames. For all stoichiometries, the burned-gas concentrations of the major species CO, O_2, and CO_2 are seen to be in good agreement with those obtained from the short mechanism, whereas the profiles of H_2O and H_2 show considerable discrepancies. These discrepancies can be explained as follows. It is seen from Figs. 2–4 that, although following closely steady states, the reaction intermediates OH, H, and HO_2 attain concentrations whose order is comparable to that of the nonsteady-state species H_2 and H_2O. In the case of the two-step mechanism there are no sinks for H atoms other than molecular hydrogen and water and, therefore, element conservation dictates that the H atoms initially introduced into the system through the H_2 and H_2O contained in the fresh, unburned mixture are, in the course of combustion in the flame, merely redistributed between these two species. Therefore, if the two-step mechanism is used, too high concentrations of H_2 and H_2O are predicted within the flame resulting in a distortion of the heat-release profile and hence the flame structure. Shown in Fig. 8 is the heat-release profile, $-\sum_{i=1}^{N} h_i w_i$, as a function of temperature for a stoichiometric atmospheric-pressure wet CO–air flame calculated with the short mechanism (dashed line), the three-step mechanism (dotted line) and the two-step mechanism (dashed-dotted line); the solid line refers to the one-step mechanism to be derived below and, therefore, can be ignored for the moment. Note that the three-step mechanism results shown here have been obtained with the mechanism derived in Ref. 6, but with the kinetic data of Table 1. It is seen from Fig. 8 that with the three-step mechanism the region of heat release in the flame, and hence the flame itself, is thinner than with the short mechanism, and that this is even more pronounced with the two-step mechanism. Furthermore, it is seen that the more the short mechanism is reduced, the more the heat release occurs at higher temperatures, but in a manner such that the overall heat release, which can be interpreted as the area under the

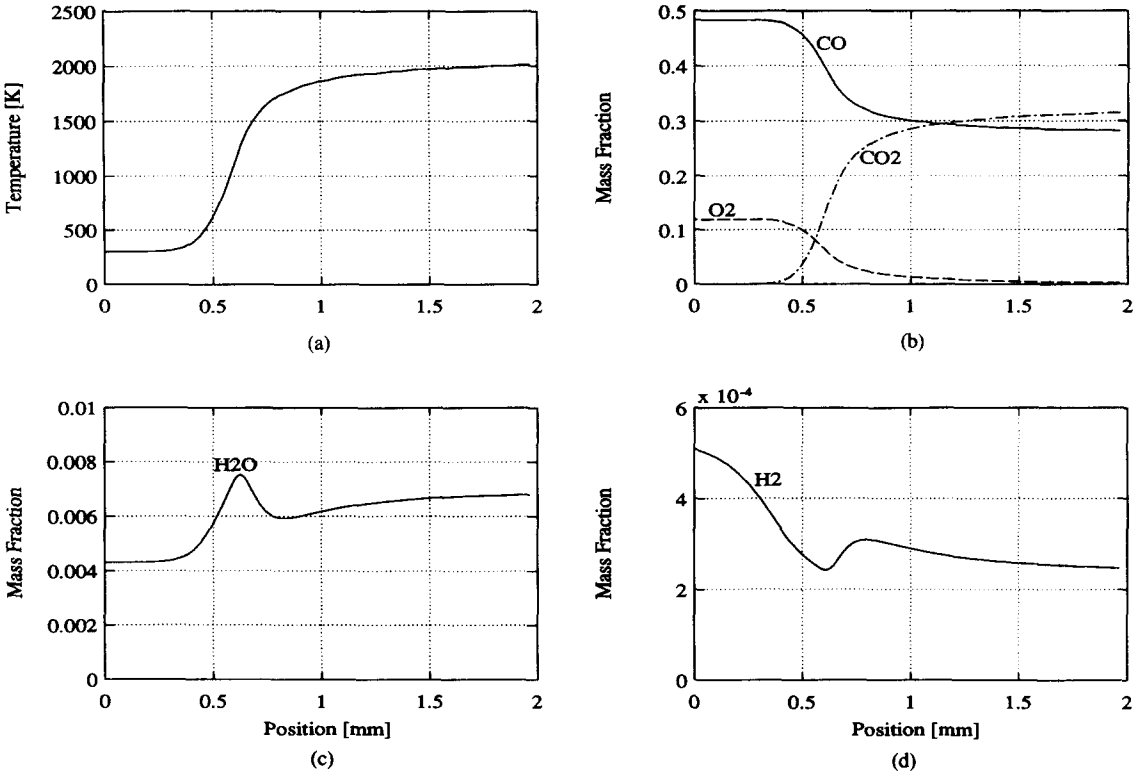

Fig. 6. As Fig. 5, but with an initial mole fraction of fuel of 0.5.

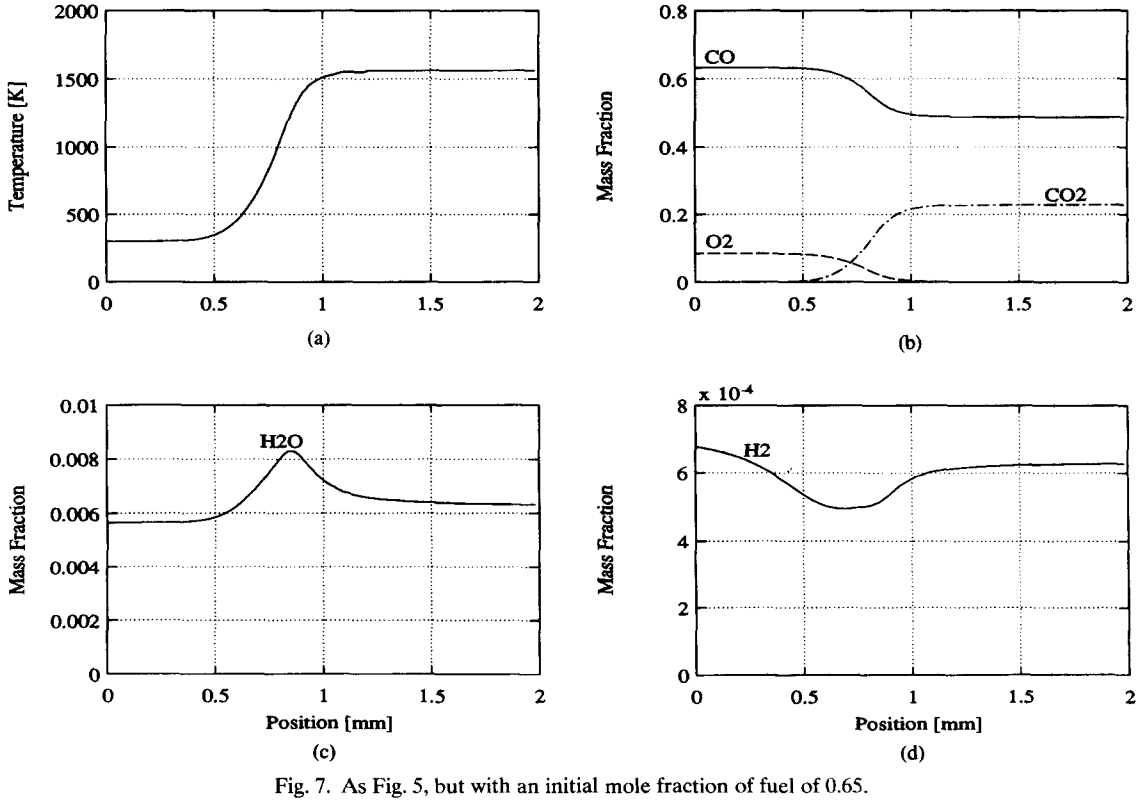

Fig. 7. As Fig. 5, but with an initial mole fraction of fuel of 0.65.

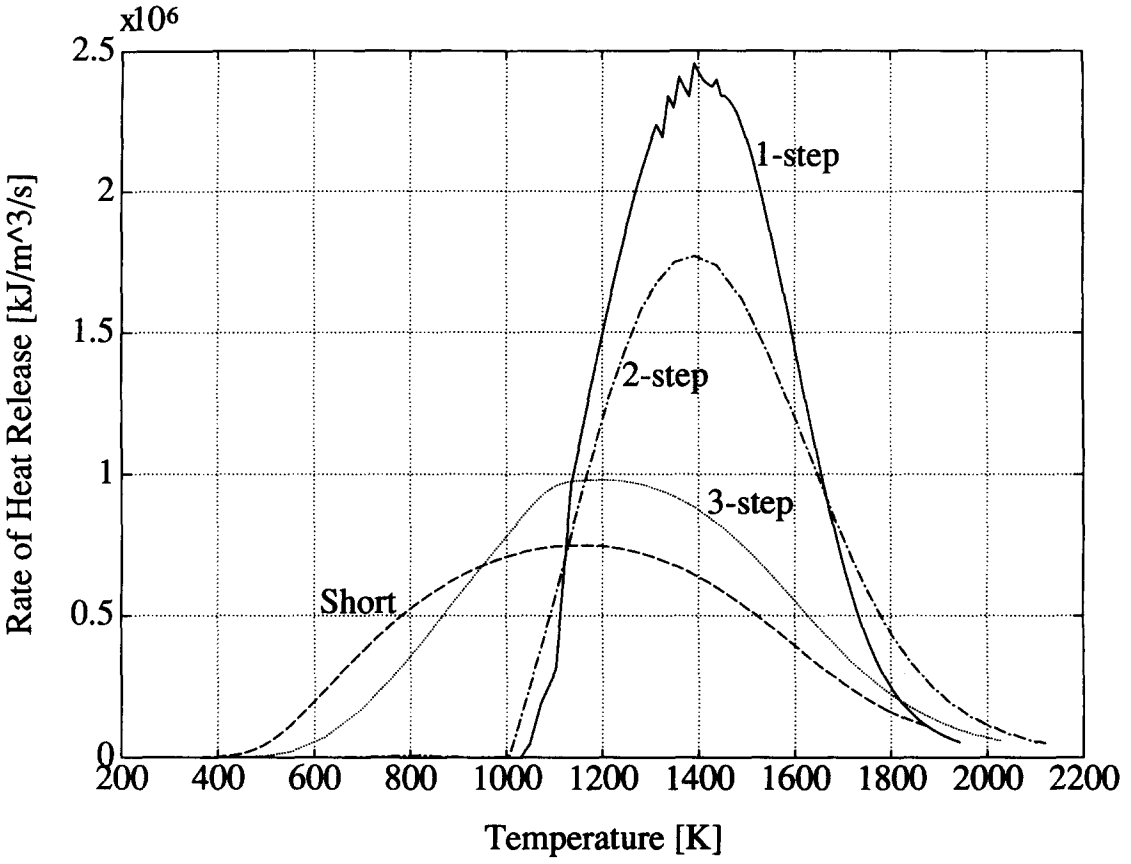

Fig. 8. Profile of the heat-release rate, $-\Sigma_{i=1}^{N} h_i w_i$, as a function of temperature for a stoichiometric atmospheric-pressure wet CO–air flame calculated with the short mechanism (dashed line), the three-step mechanism (dotted line), two-step mechanism (dashed-dotted line) and one-step mechanism (solid line), respectively.

heat-release profile, is approximately the same for all mechanisms. The latter observation is consistent with the good agreement of the burning velocities predicted by the different mechanisms. Furthermore, with regard to Fig. 8, we draw attention to the abrupt ceasing of heat release when the temperature drops below approximately 1050 K, an observation which relates directly to the principle of cutoff temperature to be employed below in the derivation of a one-step mechanism.

Two further points are worth noting. Firstly, increasing the initial CO and, hence, H_2 and H_2O mole fractions gives rise to concentrations of H_2 and H_2O in the flame that substantially exceed the concentrations of the H-atom containing reaction intermediates. As a consequence, elimination of the latter species from the mechanism leads to less severe redistribution of H-atoms on H_2 and H_2O thereby resulting in a better prediction of the concentrations of the latter species, see Fig. 7. Secondly, we note that the quality of the H_2 and H_2O concentrations as predicted with the two-step mechanism could be improved by introducing ad-hoc corrections in a manner similar to the ones employed in Ref. 28. However, such corrections are not introduced here. Instead, we choose to eliminate H_2 and H_2O all together by reducing the two-step mechanism even further, that is, to a one-step kinetic approximation.

7. A ONE-STEP MECHANISM

For many applications of practical interest it is sufficient to predict accurately the burning velocity and the flame structure in terms of temperature and major species concentrations. Hence it is desirable to have available a one-step kinetic description of the flame chemistry. The physicochemical basis of and prospects for

such a description were discussed in detail in a previous paper [6] and, therefore, are not repeated here. Instead, we proceed straight to the heart of the matter, that is, the derivation of a one-step chemistry description that will be shown to give good results for the burning velocity and the flame structure over a wide range of stoichiometries.

Derivation of the One-Step Mechanism

Taking the above two-step mechanism as a starting point, a one-step chemistry description for wet CO flames is readily obtained by assuming additional steady states for H_2 and H_2O. Specifically, by use of the steady-state relationships for the latter species,

$$0 = \omega_{2f} - \omega_{2b} + \omega_{3f} - \omega_{3b} - \omega_7 - \omega_{15} - \omega_{21}, \quad (21)$$

$$0 = \omega_{3f} - \omega_{3b} + \omega_{4f} - \omega_{4b} + \omega_8 + \omega_9 + \omega_{16}, \quad (22)$$

and of Eqs. 9–13 it is easily shown that the one-step reaction

$$CO + \frac{1}{2}O_2 \rightarrow CO_2 \quad (I'')$$

results, whose rate ω is

$$\omega = \omega_{18f} - \omega_{18b}. \quad (23)$$

Although derivation of reaction (I'') and its rate ω, Eq. 23, is a straightforward matter, the task to express ω in terms of the temperature and the concentrations of the steady-state species is neither trivial nor unique. Approximations that accomplish this remaining task are discussed in the following subsections.

7.2. Validity of the Steady-State Approximation for H_2 and H_2O

The importance of the competition for the H atom between steps $1f$ and $5f$, and under fuel-rich conditions step 21, was discussed previously [6]. In particular, it was established that because of the appreciable activation energy of step $1f$ and the zero activation energy of steps $5f$ and 21, there is a critical temperature T_c, termed "cutoff" or "crossover" temperature, below which radical production through step $1f$ is negligible compared with radical removal through steps $5f$ and 21.

For temperatures greater than T_c it is found that the steady states for H_2 and H_2O are good. From Eqs. 21 and 22, the steady-state concentrations of these species can be written as

$$[H_2] = \frac{k_{3b}[H][H_2O] + k_7[H][HO_2] + k_{21}[H][HCO]}{k_{3f}[OH]}, \quad (24)$$

$$[H_2O] = \frac{k_{4f}[OH]^2 + k_8[OH][HO_2]}{k_{3b}[H] + k_{4b}[O]}. \quad (25)$$

In writing Eqs. 24 and 25, certain elementary steps have been neglected. Specifically, in the steady state for H_2 ω_{2f}, ω_{2b}, and ω_{15} have been truncated, in that for H_2O ω_{3f}, ω_9, and ω_{16}. We point out that, as usual in the derivation of reduced kinetic mechanisms, these truncations are the result of carefully conducted numerical experiments and sensitivity analyses that were performed with the aim to achieve algebraic simplifications in the steady-state expressions and, simultaneously, to retain the quality of the predictions of burning velocity and flame structure over a wide range of stoichiometries.

For temperatures less than T_c it is found that the steady states for H_2 and H_2O break down. Therefore, for $T < T_c$, rather than by assuming steady states for H_2 and H_2O, algebraic simplifications are achieved by taking these species as inerts with constant Lewis numbers and by assuming that there is no net heat release. That the latter assumption is justified may be concluded by inspecting in Fig. 8 the heat-release profile obtained for the two-step mechanism (dashed-dotted line) in whose derivation no cut-off temperature has been employed. The heat-release profile obtained for the one-step mechanism, which we are about to derive, is included in Fig. 8 as the solid line. As discussed above in the context of the two-step mechanism, it is seen that the area under the heat-release profiles obtained with the different mechanisms is

approximately the same implying approximately equal overall heat release.

With the assumption of negligible chemical reaction for $T < T_c$, the species conservation equations for H_2 and H_2O and the energy equation can be integrated analytically to give, after elimination of the spatial coordinate,

$$\frac{[H_2]}{\rho} = \frac{[H_2]_u}{\rho_u} + \left(\frac{[H_2]_c}{\rho_c} - \frac{[H_2]_u}{\rho_u}\right) \times \left(\frac{T - T_u}{T_c - T_u}\right)^{L_{H_2}}, \quad (26)$$

$$\frac{[H_2O]}{\rho} = \frac{[H_2O]_u}{\rho_u} + \left(\frac{[H_2O]_c}{\rho_c} - \frac{[H_2O]_u}{\rho_u}\right) \times \left(\frac{T - T_u}{T_c - T_u}\right)^{L_{H_2O}}, \quad (27)$$

where the subscripts u and c identify the values at the cold boundary and temperature-crossover position in the flame, respectively. The numerical values of the Lewis numbers are 0.2625 for H_2 and 0.9230 for H_2O. Note that the concentrations of H_2 and H_2O and the density at the crossover temperature T_c, as well as T_c itself, are unknown; these quantities are determined as part of the solution.

Following [6], an approximation to the crossover temperature T_c for cutoff of branching is obtained by equating the rates of steps $1f$ and $5f$; the rate of step 21 is neglected here to achieve greater algebraic simplifications. If step 21 is taken into account, T_c is found to increase somewhat with increasing X_{CO}, but the increase is always small enough to safely be neglected. Thus, at T_c, the approximate equality

$$k_{1f} \approx k_{5f}[M] \quad (28)$$

is applied which, assuming equal third-body efficiency of unity for all species and given pressure, is readily solved for T_c. We note that T_c can be determined prior to a flame computation. To start the numerical solution of a flame from scratch, as initial estimates for ρ_c, $[H_2]_c$ and $[H_2O]_c$ to be employed in Eqs. 26 and 27 we use the ad hoc relationships

$$\rho_c = f_\rho \rho_u,$$
$$[H_2]_c = f_{H_2}[H_2]_u, \quad (29)$$
$$[H_2O]_c = f_{H_2O}[H_2O]_u,$$

with $f_\rho = 0.254$, $f_{H_2} = 0.078$ and $f_{H_2O} = 0.618$. The numerical values for f_ρ, f_{H_2}, and f_{H_2O} were estimated from calculated flame-structure results obtained with the short mechanism. It has been found, however, that the efficiency of the overall numerical solution method is quite insensitive to the initial guesses for ρ_c, $[H_2]_c$, and $[H_2O]_c$.

By using the technique of inner iteration, which is described in detail in subsection 7.4, improved values for ρ_c, $[H_2]_c$, and $[H_2O]_c$ are calculated as the solution to the overall problem is approached. Specifically, at each inner-iteration sweep over all gridpoints, values for ρ_c, $[H_2]_c$, and $[H_2O]_c$ obtained from the previous sweep are used.

7.3. Truncation of the Steady-State Relationships

For the derivation of a good one-step kinetic description, different kinetic approximations need to be introduced than for the two-step mechanism. In particular, the one-step mechanism requires different truncations in the steady-state relationships than the two-step mechanism. Based on extensive numerical explorations it has been found that for the above one-step reaction over a wide range of stoichiometries the best burning velocities and flame structures are obtained if for H_2 and H_2O the truncations described above are introduced together with the following truncations for the remaining steady-state species: in the steady state for H atoms, ω_{3f}, and ω_{24f} are to be truncated; in that for the OH radical, ω_{10}; in that for O atoms, ω_9 and ω_{10}; in that for the HO_2 radical, ω_6; in that for HCO, no truncations are to be made. The steady-state relationships can be solved for the concentrations of the steady-state species. The resulting relationships are Eqs. 24 and 25 for H_2 and

H_2O, respectively, and

$$[OH] = \frac{N}{D}, \tag{30}$$

$$N = k_{1f}[H][O_2] + k_{2f}[H_2][O] + k_{3b}[H][H_2O] + 2k_{4b}[H_2O][O] + 2k_6[H][HO_2] + k_{18b}[CO_2][H],$$

$$D = k_{1b}[O] + k_{2b}[H] + k_{3f}[H_2] + 2k_{4f}[OH] + k_8[HO_2] + k_{16}[H][M] + k_{18f}[CO],$$

$$[H] = \frac{N}{D}, \tag{31}$$

$$N = k_{1b}[O][OH] + k_{2f}[H_2][O] + k_{18f}[CO][OH],$$

$$D = k_{1f}[O_2] + k_{2b}[OH] + k_{3b}[H_{2O}] + k_{5f}[M][O_2] + k_6[HO_2] + k_7[HO_2] + k_9[HO_2] + 2k_{15}[H][M] + k_{16}[M][OH] + k_{18b}[CO_2] + k_{21}[HCO] + k_{24b}[CO][M],$$

$$[HO_2] = \frac{k_{5f}[H][O_2][M]}{k_7[H] + k_8[OH] + k_9[H] + k_{10}[O]}, \tag{32}$$

$$[O] = \frac{k_{1f}[H][O_2] + k_{2b}[H][OH] + k_{4f}[OH][OH]}{k_{1b}[OH] + k_{2f}[H_2] + k_{4b}[H_2O]}, \tag{33}$$

$$[HCO] = \frac{k_{24b}[CO][H][M]}{k_{21}[H] + k_{24f}[M]} \tag{34}$$

for the remaining steady-state species. It is seen that Eqs. 30–34, 24, and 25 are strongly coupled and, therefore, must be solved by means of inner iteration. The general principles of inner iteration are discussed in the present paper in section 4 and, more specific to premixed ethane and ethylene flames, in Ref. 24; inner iteration for the wet CO flames based on the above one-step mechanism is described in the following subsection.

7.4. Inner Iteration

For a steady-state species i, the species conservation Eq. 2 reduces to $w_i = 0$. Thus, for a steady-state species the convective and diffusive terms, which for evaluation at a specified gridpoint require information from neighboring points, are absent in the species conservation equation. As a consequence, assuming that the temperature and the concentrations of the nonsteady-state species are known by solving the governing equations, in the present paper Eqs. 1 and 2, the solution of the steady-state relationships at any gridpoint of the computational domain is independent of the solution of these relationships at the remaining gridpoints. In this sense, inner iteration is applied *pointwise*. In the present paper we determine the steady-state concentrations from left to right, that is, we begin with inner iteration at the leftmost gridpoint, which corresponds to the cold boundary, and, once steady-state concentrations have been determined at this point, start a new inner iteration at the second grid point, and so on.

Shown in Fig. 9 is a flowchart illustrating inner iteration for wet CO–air flames with the one-step kinetic mechanism. In this chart "input" means that the temperature and the concentrations of the species appearing explicitly in the reduced mechanism are considered as known quantities. Prior to entering the inner-iteration cycle at any gridpoint, the following initial values are assigned to the concentrations of the steady-state species: at the cold boundary, that is, gridpoint 1, [OH], [H], [HO_2], [O], and [HCO] are taken as zero, and [H_2] and [H_2O] are obtained from the relationships $[H_2] = (X_{H_2,u}/X_{CO,u})$ [CO] and $[H_2O] = (X_{H_2O,u}/X_{CO,u})$ [CO], respectively. For the flames considered in the present paper we have $X_{H_2,u}/X_{CO,u} = 0.015$ and $X_{H_2O,u}/X_{CO,u} = /0.0135$. Then the inner-iteration cycle is entered. At gridpoint $l, 2 \le l \le l_c$, where l_c denotes the number of the gridpoint at which the crossover temperature is imposed, [H_2] and [H_2O] are calculated from Eqs. 26 and 27,

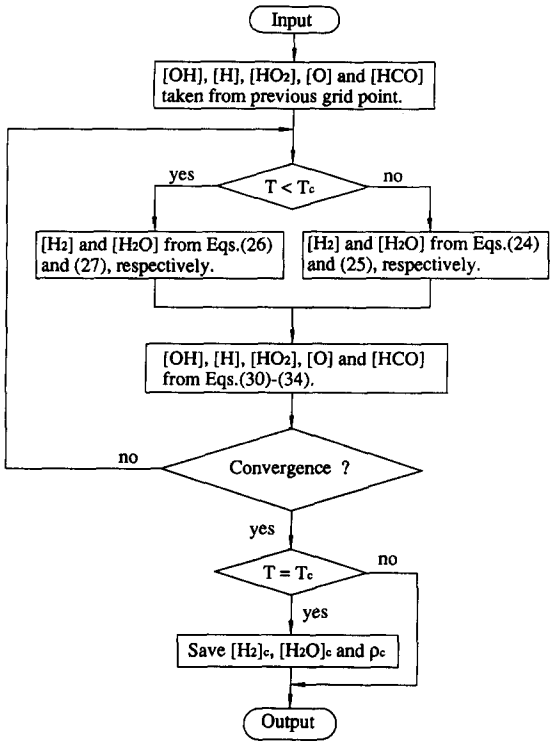

Fig. 9. Flowchart illustrating inner iteration for a wet CO–air flame calculated with the one-step reduced kinetic mechanism.

respectively. Note that the latter two equations can be solved explicitly for $[H_2]$ and $[H_2O]$. At gridpoint $l, l > l_c$, $[H_2]$ and $[H_2O]$ are calculated from Eqs. 24 and 25. In the first inner-iteration step, for the $[H_2]$ and $[H_2O]$ appearing on the right hand sides of Eqs. 24 and 25 the converged values at gridpoint $l - 1$ are adopted. In the second and later inner-iteration steps, for the $[H_2]$ and $[H_2O]$ appearing on the right hand sides of Eqs. 24 and 25 the respective values obtained in the previous inner-iteration step at gridpoint l are adopted. Once the iterative values for $[H_2]$ and $[H_2O]$ have been obtained, iterative values for [OH], [H], $[HO_2]$, [O], and [HCO] are obtained from Eqs. 30–34. This is followed by a check for convergence of the inner iteration. If convergence has not yet been achieved, the next inner-iteration step is started. Note that if the gridpoint under consideration is the crossover point c, the converged concentrations of H_2 and H_2O together with the density are saved so that they are available at the next inner-iteration sweep over all grid points; see at the end of subsection 7.2. Finally, "output" in the flowchart means that now all the concentrations of those intermediate species, which are required to evaluate the global reaction rate, that is, the right hand side of Eq. 23, are available.

From the flowchart it is obvious that inner iteration can be performed in a "black box" to which input is supplied in terms of temperature and concentrations of those species which appear explicitly in the reduced mechanism, and which provides output in terms of the concentrations of the intermediate species which do *not* explicitly appear in the mechanism. Black boxes of inner iteration as just identified are desirable from the engineering point of view where the primary concern is the *application* of reduced kinetic mechanisms to combustion systems rather than their derivation. The construction of numerically reliable and robust black-box inner iterations is a topic of ongoing research.

7.5. Results for the One-Step Mechanism

Included in Fig. 1 as solid lines are burning velocities obtained with the above one-step mechanism for different initial concentrations of fuel and oxidizer. It is seen that the burning velocities calculated with the one-step mechanism are in good agreement with those obtained with the detailed mechanisms and the two-step mechanism if the oxidizer contains appreciable amounts of nitrogen, that is, for $f = 0.13$, 0.21, and 0.4. However, for low amounts of nitrogen in the oxidizer, for example, for $f = 0.985$, for moderately lean to stoichiometric flames the one-step reduced mechanism gives higher burning velocities than the short or detailed mechanism. For lean flames at $f = 0.985$ it has been found that the burning velocity is not unique. Specifically, for identical sets of parameters, that is, for one and the same flame, different burning velocities are predicted if the numerical-solution procedure is started with different initial profiles. This indicates the limitations of the one-step approximation.

Shown in Fig. 10 are numerical results for flame structures of a wet CO–air flame ($f = 0.21$) obtained with the above one-step mecha-

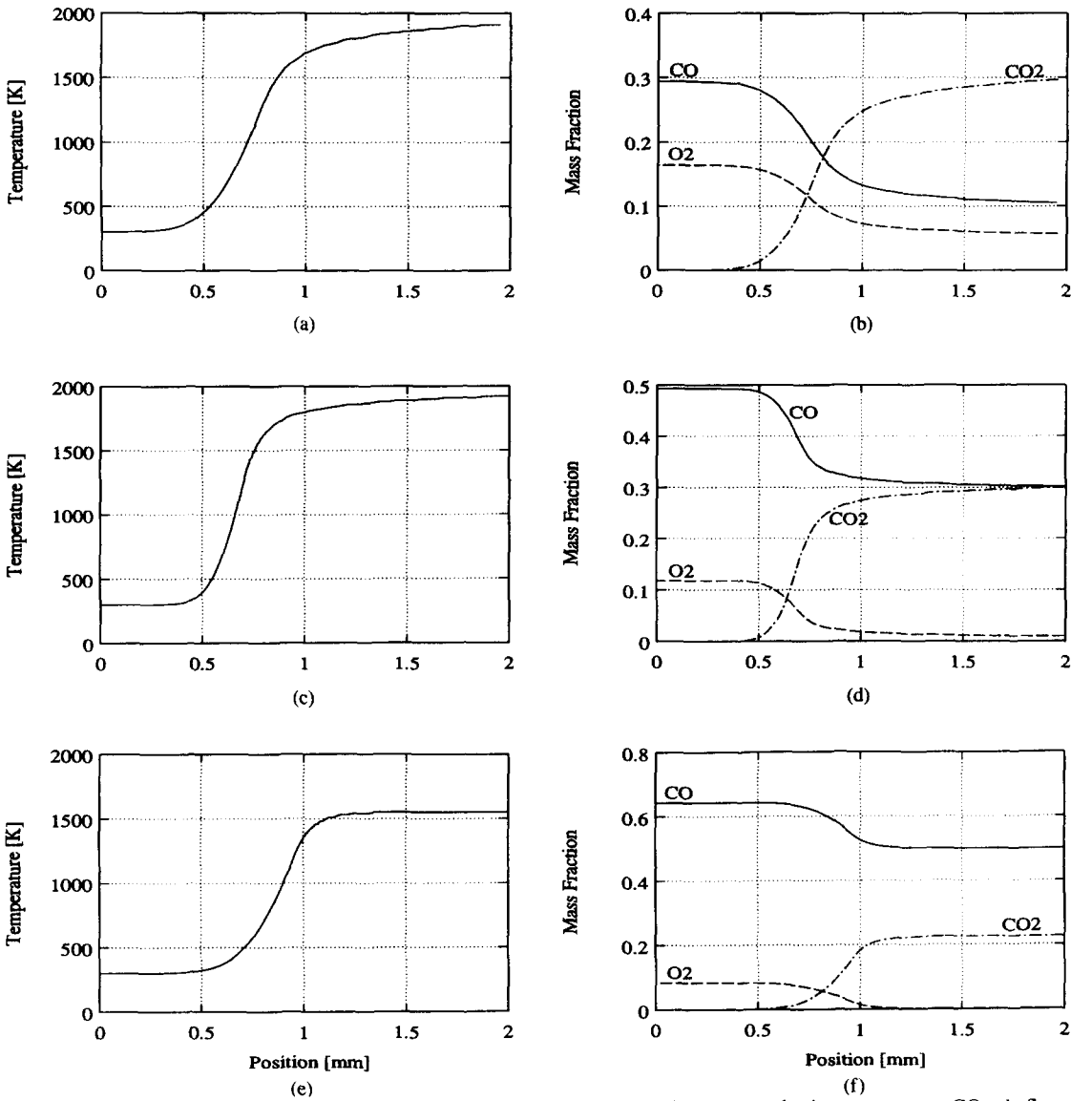

Fig. 10. Temperature and mass-fraction profiles of CO, O_2, and CO_2 for three atmospheric-pressure wet CO–air flame calculated with the one-step kinetic approximation. (a) and (b) are for $X_{CO} = 0.3$, (c) and (d) for $X_{CO} = 0.5$, and (e) and (f) for $X_{CO} = 0.65$.

nism. Figures 10a and 10b pertain to a near-stoichiometric flame with initial CO mole fraction $X_{CO} = 0.3$, Figs. 10c and 10d to a moderately rich flame with $X_{CO} = 0.5$, and Figs. 10e and 10f to a very rich flame with $X_{CO} = 0.65$. It is seen from Fig. 10 that, although the moderately rich to very rich flames calculated with the one-step reduced mechanism are thinner than those calculated with the detailed mechanisms or the two-step mechanism, the maximum temperature and the concentrations of the products are well predicted by the one-step mechanism.

8. TRICKS FOR CALCULATIONS WITH REDUCED MECHANISMS

In this section we summarize a few findings that we have found useful to employ in numerical calculations with reduced mechanisms. Some of these findings are specific to the wet CO flames investigated in the present paper,

others are of more general nature. However, even the specific findings may be useful for future work and, therefore, they are reported here. The more general findings that we report reflect the experience made by the authors in the area of flame-structure computations with systematically reduced kinetic mechanisms over an extended period of time.

As discussed in section 4 and subsection 7.4, the calculation of concentrations of steady-state species in the course of the computational solution of a combustion problem often requires a numerical process called "inner iteration." In general, not only does the rate of convergence towards the numerical solution of the combustion problem at hand depend strongly on the details of the inner iteration but, if the inner iteration is constructed in an unsuitable manner, a converged numerical solution to the combustion problem may not be obtainable at all.

Specifically for the wet CO flames based on the one-step kinetic approximation developed above, the governing equations together with Eqs. 24–27 and 30–34 form a complicated system. Since the concentrations of all H-containing species, however small in value, are calculated from the "primary variables" [CO], $[O_2]$, and $[CO_2]$ and T that appear explicitly in the one-step mechanism and, hence, the governing equations, the primary variables have a strong influence on the concentrations predicted for the steady-state species, and vice versa. In particular, any tiny deviation of an intermediate-species solution, which often occurs in the course of an iterative overall solution, might be exaggerated by the H_2–O_2 system that, implicitly, is described totally by Eqs. 26, 27, and 30–34, and, thereby, lead to divergence of the overall solution procedure. Of critical importance in obtaining a converged solution for the wet CO flame with one-step chemistry are the treatment of the steady-state concentrations in the vicinity of the crossover temperature. Details of this treatment are discussed in the following subsection.

8.1. Crossover Temperature

For given pressure, the crossover temperature T_c can be calculated straightforwardly from Eq. 28. This fact is deceptive, however, since in the vicinity of T_c the concentrations of the steady-state species vary extremely strongly with temperature. In particular, the steady-state approximations for H_2 and H_2O break down in an asymptotically thin layer around T_c. As a consequence, during the initial stage of the computation of a wet CO flame with one-step chemistry, small errors in the temperature profile around T_c may lead to physically meaningless values of the concentrations of the steady-state species that slow down the rate of convergence of the numerical method or even lead to divergence. To overcome this problem the following trick has successfully been employed. During the initial stage of the computation a value for T_c is chosen that is higher by, say, 50 K than the value obtained from Eq. 28. As a consequence, the steady states for H_2 and H_2O are applied only further downstream, that is, in portions of the flame sufficiently "remote" from that location where the steady states for these species break down. This "remoteness" gives more flexibility to the numerical method, that is, the domain of convergence of the numerical method is increased and, hence, the chances of obtaining a converged numerical solution are increased. Once in a first run a converged numerical solution has been obtained, in successive runs the artificially increased crossover temperature is reduced stepwise until a converged solution for the real crossover temperature given by Eq. 28 is obtained.

8.2. Avoiding Zero Denominators

A potential problem with the use of systematically reduced kinetic mechanisms is the appearance in expressions of denominators that may be, or approach, zero. An example is

$$[\mathscr{M}_i] = \frac{N}{D}, \tag{35}$$

where $[\mathscr{M}_i]$ is the concentration of a steady-state species, say, or any other fractional expression, and where N and D denote the numerator and denominator of the expression, respectively. It is important to note that, in general, N and D are functions of temperature and concentrations of both non-steady-state and steady-state species.

In general, if a denominator approaches zero so does the numerator, and the fractional expression has a well defined finite value. An approach to overcome the zero-denominator problem that, though not reliable is often used, is to replace concentrations that approach zero by a small but finite value ϵ, that is, to replace Eq. 35 by

$$[\mathcal{M}_i] = \frac{N}{\max(D, \epsilon)}. \tag{36}$$

However, inner iteration allows the zero-denominator problem to be overcome without ad-hoc corrections of the kind used in Eq. 36 in the following manner. Any expression of the form of Eq. 35 can be rewritten as

$$[\mathcal{M}_i] = \frac{N + \epsilon[\mathcal{M}_i]}{D + \epsilon}, \tag{37}$$

and then, simultaneously with the steady-state relationships, be subjected to the inner-iteration. The obvious advantages of Eq. 37 over Eq. 35 and 36 are (1) that, if a proper value of ϵ is selected, a numerical zero of the denominator will never occur, and (2) that it is exact. In our computations we have found that values of ϵ work well that satisfy the relationship

$$\epsilon_{\min} \leq \epsilon \leq \epsilon_{\max}. \tag{38}$$

Here $\epsilon_{\min}$ is approximately 10 to 100 times the smallest positive number that the computer recognizes, and $\epsilon_{\max}$ is approximately 10–100 times the minimum value of $[\mathcal{M}_i]$ found in the flame.

8.3. Partially Explicit Numerical Schemes

The usefulness of Newton's method in its present form, in which it has been used by many research groups to solve a variety of combustion problems using detailed kinetic mechanisms of elementary reactions, as the ideal solution method with systematically reduced kinetic mechanisms was questioned previously [29, 30]. Therefore, we now present the so-called partially explicit numerical approach to the solution of combustion problems with reduced mechanisms based on inner iteration. We note that the application of the partially explicit approach is not restricted to the Newton method but can be used in conjunction with many other numerical schemes.

8.3.1. The Partially Explicit Newton Method for Steady Flames

The partially explicit Newton method for steady flames results if in the Jacobian matrix those elements are neglected that are related to steady-state and partial equilibrium relationships that require inner iteration for their solution. In practice this verbally "easy" statement can be realized as follows.

Newton's method is applied to the system of nonlinear equations

$$\mathbf{F}(\mathbf{U}) = \mathbf{0}, \tag{39}$$

which results from the discretization of the governing equations on a nonuniform grid; here $\mathbf{U}$ denotes the vector of unknowns. Thus the linear system

$$J(\mathbf{U}^k)(\mathbf{U}^{k+1} - \mathbf{U}^k) = -\omega_k \mathbf{F}(\mathbf{U}^k), \qquad k = 0, 1, \ldots \tag{40}$$

is solved, where $\mathbf{U}^k$ denotes the solution after k Newton iterations, and ω_k and $J(\mathbf{U}^k)$ are the damping parameter and the Jacobian matrix, respectively, based on $\mathbf{U}^k$.

For the original fully implicit Newton method with reduced kinetic mechanisms, the unknown vector $\mathbf{U}$ can be expressed as

$$\mathbf{U} = \mathbf{U}(T, Y_i) = \mathbf{U}\big(T, Y_i; C_j(T, Y_i)\big). \tag{41}$$

Here the temperature T and the mass fractions Y_i, $i = 1, \ldots, N$, of the major species all appear explicitly in the governing equations. The concentrations C_j of the steady-state species, which are needed to calculate the global rates, are functions of T and the Y_i; they do not appear explicitly in the governing equations and, therefore, in the last expression in Eq. 41 a semicolon has been used to separate the $C_j(T, Y_i)$ from the other arguments.

A partially explicit formulation of the Newton method can be realized by writing the vector of unknowns as

$$\mathbf{U} = \mathbf{U}(T, Y_i) = \mathbf{U}\big(T, Y_i; C_j\big(T^k, Y_i^k\big)\big), \tag{42}$$

where T^k and Y_i^k, $i = 1, \ldots, N$, are the temperature and major-species mass fractions of the last *successful* Newton-iteration step. It is worthwhile to discuss in somewhat greater detail the fine difference between Eqs. 41 and 42. For instance, Eqs. 41 and 42 give *identical* results for the residual vector $\mathbf{F}(\mathbf{U}^k)$, $k = 0, 1, \ldots$, which appears on the right-hand side of Eq. 40, when $\mathbf{F}(\mathbf{U}^k)$ is updated after a successful Newton-iteration step. On the other hand, Eqs. 41 and 42 give *different* results for the Jacobian matrix $J(\mathbf{U}^k)$, $k = 0, 1, \ldots$, which appears on the left-hand side of Eq. 40, if $J(\mathbf{U}^k)$ is calculated by numerical differentiation. This is so because numerical differentiation involves the component-wise incrementation of $\mathbf{U}^k$, and, in general, the incremented $\mathbf{U}^k$ based on Eq. 41 is different from the incremented $\mathbf{U}^k$ based on Eq. 42. Although superficially the difference between Eqs. 41 and 42 seems to be marginal, it has been found that Eq. 42 improves convergence of the Newton method compared to Eq. 41. In extreme cases Eq. 42 helped to obtain converged results where Eq. 41 failed. Finally we note that inner iteration alone is equivalent to the definition of $\mathbf{U}$ given in Eq. 41, that is, inner iteration does *not* render the Newton method partially explicit.

8.3.2. Partially Explicit Numerical Schemes for Unsteady Flames

An alternative approach to obtain the solution to a steady combustion problem by solving the steady version of the governing equations is to solve the time-dependent version of these equations until a steady solution is reached. Explicit numerical schemes for the solution of unsteady combustion problems do not require any modifications when applied in conjunction with a systematically reduced kinetic mechanism based on inner iteration. They do, however, suffer from the well-known severe restrictions on the possible size of the time step.

Implicit numerical schemes for the solution of unsteady combustion problems, such as Newton's method applied at each time step to the set of unsteady governing equations, are readily rendered partially explicit for use in conjunction with a systematically reduced kinetic mechanism based on inner iteration by evaluating at each time step the concentrations of the steady-state species with values from the previous successful time step. We note that implicit numerical schemes for the solution of unsteady combustion problems can be more easily prepared for use with reduced kinetic mechanisms than partially explicit schemes operating on the steady versions of the governing equations; on the other hand, when steady-state solutions to the governing equations are sought, the latter schemes are more economical to use than the former.

9. RANGES OF VALIDITY, RECOMMENDATIONS

At this stage it appears worthwhile to summarize the ranges of validity for the various mechanisms derived and/or employed in the present work.

Both the full detailed and short detailed kinetic mechanism have been tested not only for the wet CO flames investigated in the present article, but for a variety of other problems such as counterflow diffusion flames, [19]. Since the kinetics of $CO-H_2-N_2$ systems are well understood, the two detailed mechanisms can be regarded as "safe" with respect to their applicability over wide ranges of temperatures, stoichiometries and pressures, although some care must be taken if the short mechanism is applied to extreme situations where the neglected steps, that is, the steps whose numbers are given in parentheses in Table 1 become important.

The three-step, two-step and one-step mechanism presented herein have been derived for laminar, premixed flames only and, therefore, cannot be expected to be suitable for application to diffusion-flame problems. Nevertheless, it is worth noting that Chen et al. [27] have used successfully the three-step mechanism derived by Rogg and Williams for premixed wet CO flames [6] to simulate laminar diffusion flames. Similarly, Peters and Kee [31] have successfully simulated laminar methane–air diffusion flames using a four-step mechanism derived by Peters [32] for premixed flames. The mechanisms derived herein have been derived for specific values of initial temperature

(300 K) and pressure (1 bar), and for specified ranges of initial composition and, therefore, can be used with confidence under similar conditions. In particular, the mechanisms have been derived for conditions where only small amounts of hydrogen and water are added to the initial carbon monoxide. The one-step mechanism should be used with caution for only weakly nitrogen-diluted flames.

We recommend that either the three-step mechanism, for instance in the formulation of Rogg and Williams [6], or, alternatively, the one-step mechanism derived herein should be used. Use of the two-step mechanism is not encouraged because of the possible overprediction of H_2 and H_2O in the hot portion of a flame. The one-step mechanism has the advantage of greatest computational efficiency, the three-step mechanism that of providing information on additional species which are not contained in the one-step mechanism.

10. CONCLUSIONS

Wet CO flames are interesting testing grounds for reduced mechanisms because of the initial anticipation of being able to achieve a good one-step approximation. In the present article, it has been shown that this anticipation indeed is justified. To this end, first, an excellent short detailed mechanism was identified here. This mechanism was then reduced successively to a global three-step, two-step and, finally one-step mechanism. All reduced mechanisms are found to give good results for the burning velocity and flame structure over a wide range of stoichiometries. Limitations of the one-step mechanism occur for weakly nitrogen-diluted flames.

Due to the reduced number of chemical species appearing in reduced kinetic mechanisms, such mechanisms are anticipated to be more cost-effective in numerical calculations than comparable calculations with detailed mechanisms of elementary reactions, provided, of course, the reduced mechanisms are numerically tractable. Therefore, herein we have summarized tricks for flame computations with reduced mechanisms that help to overcome specific numerical difficulties than can occur, thereby contributing to increased, overall usefulness of reduced kinetic mechanism in general combustion modelling and simulation. Finally, the ranges of validity of the derived mechanisms have been summarized and recommendations as to which mechanism to use have been given.

This work was supported by NATO through Grant No. 0102 / 89. The authors would like to thank Professor F. A. Williams for stimulation and helpful comments.

REFERENCES

1. Lewis, B., and von Elbe, G., *Combustion, Flames and Explosions of Gases*, 3rd ed., Academic, Orlando, 1987.
2. Warnatz, J., *Ber. Bunsenges. Phys. Chem.* 83:950–957 (1979).
3. Cherian, M. A., Rhodes, P., Simpson, R. J., and Dixon-Lewis, G., *Eighteenth Symposium (International) on Combustion*, The Combustion Institute, Pittsburgh, 1981, pp. 385–396.
4. Cherian, M. A., Rhodes, P., Simpson, R. J., and Dixon-Lewis, G., *Philos. Trans. R. Soc. Lond. A*, 303(1476):181–212 (1981).
5. Dixon-Lewis, G., *Proc. R. Soc. Lond. A* 330:219–245 (1972).
6. Rogg, B., and Williams, F. A., *Twenty-Second Symposium (International) on Combustion*, The Combustion Institute, Pittsburgh, 1988, pp. 1441–1451.
7. Wang, W., Rogg, B., and Williams, F. A., in *Reduced Kinetic Mechanisms for Applications in Combustion Systems* (N. Peters and B. Rogg, Eds.), Springer, Berlin, 1993, pp. 44–57.
8. Rogg, B., *Combust. Flame* 73:45–65 (1988).
9. Hirschfelder, J. O., and Curtiss, C. F., in *Third Symposium on Combustion and Flame and Explosion Phenomena*, Williams & Wilkins, Baltimore, 1949, pp. 121–127.
10. García-Ybarra, P., Nicoli, C., and Clavin, P., *Combust. Sci. Technol.* 42:87–109 (1984).
11. Rogg, B., Technical Report CUED/A-THERMO/TR39, University of Cambridge, Department of Engineering, April 1991.
12. Rogg, B., in *Computers and Experiments in Fluid Flow* (G. M. Carlomagno and C. A. Brebbia, Eds.), Springer, Berlin, 1989, pp. 75–85.
13. Rogg, B., *Major Research Topics in Combustion* (M. Y. Hussaini, A. Kumar, and R. G. Voigt, Eds.), Springer, New York, 1992, pp. 70–97.
14. Liu, Y., and Rogg, B., in *Heat Transfer in Radiating and Combusting Systems* (M. G. Carvalho, F. Lockwood, and J. Taine, Eds.), Springer, Berlin, 1991, pp. 114–127.
15. Dixon-Lewis, G., Giovangigli, V., Kee, R. J., Miller, J. A., Rogg, B., Smooke, M. D., Stahl, G., and Warnatz, J. *Prog. Astronaut. Aeronaut.* 131:125–144 (1991).
16. Rogg, B., in *NUMETA 90, Numerical Methods in*

Engineering (G. N. Pande, and J. Middleton, Eds.), Elsevier, New York, 1990, vol. 2, pp. 1129–1140.
17. Rogg, B., *Computer-Methods in Applied Mechanics and Engineering 90*, 1991, pp. 659–670.
18. Bruel, P., Rogg, B., and Bray, K. N. C., in *Twenty-Third Symposium (International) on Combustion*, The Combustion Institute, Pittsburgh, 1990, pp. 759–766.
19. Chen, J.-Y., Liu, Y., and Rogg, B., in *Reduced Kinetic Mechanics for Applications in Combustion Systems* (N. Peters and B. Rogg, Eds.), Springer, Berlin, 1993, 196–223.
20. Peters, N., and Rogg, B., Eds. *Reduced Kinetic Mechanisms for Applications in Combustion Systems*, Springer, Berlin, 1993.
21. Williams, F. A., *Combustion Theory*, 2nd ed., Benjamin/Cummings, Menlo Park, 1985.
22. Dixon-Lewis, G., *Proc. R. Soc. Lond. A* 292:45–99 (1979).
23. Rogg, B., in *Mathematical Modeling in Combustion and Related Topics* (C.-M. Brauner and C. Schmidt-Laine, Eds.), Dordrecht, Martinus Nijhoff, 1988, pp. 551–560.
24. Wang, W., and Rogg, B., in *Reduced Kinetic Mechanisms for Applications in Combustion Systems* (N. Peters and B. Rogg, Eds.), Springer, Berlin, 1993, pp. 76–101.
25. Göttgens, J., and Terhoeven, P., in *Reduced Kinetic Mechanisms for Applications in Combustion Systems* (N. Peters and B. Rogg, Eds.), Springer, Berlin, 1993, pp. 345–349.
26. Rogg, B., in *Reduced Kinetic Mechanisms and Asymptotic Approximations for Methane–Air Flames* (M. D. Smooke, Ed.), Springer, Berlin, 1991, pp. 159–192.
27. Chen, J.-Y., Dibble, R. W., and Bilger, R. W., *Twenty-Third Symposium (International) on Combustion*, The Combustion Institute, Pittsburgh, 1990, pp. 775–780.
28. Mauss, F., Peters, N., Rogg, B., and Williams, F. A., in *Reduced Kinetic Mechanisms for Applications in Combustion Systems* (N. Peters and B. Rogg, Eds.), Springer, Berlin, 1993, pp. 29–43.
29. Rogg, B., in *Proceedings of the 13th ICDERS Conference*, Nagoya (Japan), in press.
30. Rogg, B., Technical Report CUED/A-THERMO/TR44, University of Cambridge, Department of Engineering, August 1991.
31. Peters, N., and Kee, R. J., *Combust. Flame* 68:17–29 (1987).
32. Peters, N., *Lect. Notes Phys.* 241:90–109 (1985).

Received 9 August 1992; revised 26 February 1993